New evidence about the structure and growth of ocean island volcanoes from aeromagnetic data: The case of Tenerife, Canary Islands

Isabel Blanco-Montenegro,[1] Iacopo Nicolosi,[2] Alessandro Pignatelli,[2] Alicia García,[3] and Massimo Chiappini[2]

Received 15 April 2010; revised 16 November 2010; accepted 17 December 2010; published 10 March 2011.

[1] We present 3-D magnetic models of Tenerife based on a high-resolution aeromagnetic survey carried out in 2006. Two different inverse modeling techniques have been applied: (1) a linear method aimed at imaging lateral magnetization contacts and (2) a nonlinear method aimed at obtaining a 3-D description of deep intrusive bodies, in which a constant magnetization value characterizes the main sources. Magnetic models show that deep intrusive structures are located beneath the northern part of the island and aligned along the E-W direction. This arrangement of intrusive bodies does not support the hypothesis of a three-armed rift system that has been present since the early formation of the island. The shallow portion of the intrusive structures shows a round geometry that agrees with the previously proposed location of some of the landslide headwalls, suggesting that collapse scars have acted as preferential sites for magma upwelling. Our magnetic model probably provides the first geophysical evidence of the location of the headwall of the Icod landslide beneath the Teide-Pico Viejo complex, thus supporting the vertical collapse hypothesis for the origin of the Cañadas caldera. The largest intrusive complex is located to the northwest of Teide and Pico Viejo, revealing the presence of a very high dike density in this area. This complex probably resulted from the intrusion of magma over the span of millions of years, beginning with the early phases of basaltic shield volcanism in central Tenerife and lasting until the building of Teide and Pico Viejo stratovolcanoes.

Citation: Blanco-Montenegro, I., I. Nicolosi, A. Pignatelli, A. García, and M. Chiappini (2011), New evidence about the structure and growth of ocean island volcanoes from aeromagnetic data: The case of Tenerife, Canary Islands, *J. Geophys. Res.*, *116*, B03102, doi:10.1029/2010JB007646.

1. Introduction

[2] Tenerife is one of the seven Canary Islands, which are a volcanic archipelago located in the eastern central Atlantic (Figure 1a) and constructed on oceanic crust of Jurassic age [*Roest et al.*, 1992]. The central part of the island is occupied by a huge caldera, known as the Cañadas caldera, inside which the Teide-Pico Viejo stratovolcanic system developed. The highest point of the island, the Teide peak, reaches 3718 m above sea level and about 7000 m from the seafloor, which is more than 3000 m deep in this area.

[3] In recent years, our knowledge of the volcanic history of Tenerife has improved as a result of a considerable number of fresh geological and geophysical investigations [e.g., *Thirlwall et al.*, 2000; *Huertas et al.*, 2002; *Pous et al.*, 2002; *Guillou et al.*, 2004; *Leonhardt and Soffel*, 2006; *Coppo et al.*, 2008; *Gottsmann et al.*, 2008]. Some important issues, such as the origin of the Cañadas caldera or the interplay between giant landslides and rift zones, have been the subject of intense debate in the last 15 years [e.g., *Carracedo*, 1994; *Martí et al.*, 1996; *Martí and Gudmundsson*, 2000; *Walter*, 2003; *Walter et al.*, 2005]. The interest in this island was especially renewed in 2004, when an increase of seismic activity (Figure 1b) led some volcanologists to think that an eruption could be possible after almost a century of quiescence [*García et al.*, 2006; *Gottsmann et al.*, 2006; *Almendros et al.*, 2007].

[4] Several aspects of the growth and evolution of ocean island volcanoes still remain unclear. Rift zones have been recognized as major structural features in this kind of volcanic environment. They represent areas of major intrusive volcano growth and typically result in a morphological ridge. There are different theories about the origin of these structural elements. One theory proposes that rift zones are formed in the early phases of growth of the island and are due to the ascent of magma. This results in the symmetric fracturing of the crust along three directions that form angles of 120° [e.g., *Carracedo*, 1994]. Another theory considers

[1]Departamento de Física, Universidad de Burgos, Burgos, Spain.
[2]Istituto Nazionale di Geofisica e Vulcanologia, Rome, Italy.
[3]Departamento de Volcanología, Museo Nacional de Ciencias Naturales, CSIC, Madrid, Spain.

0148-0227/11/2010JB007646

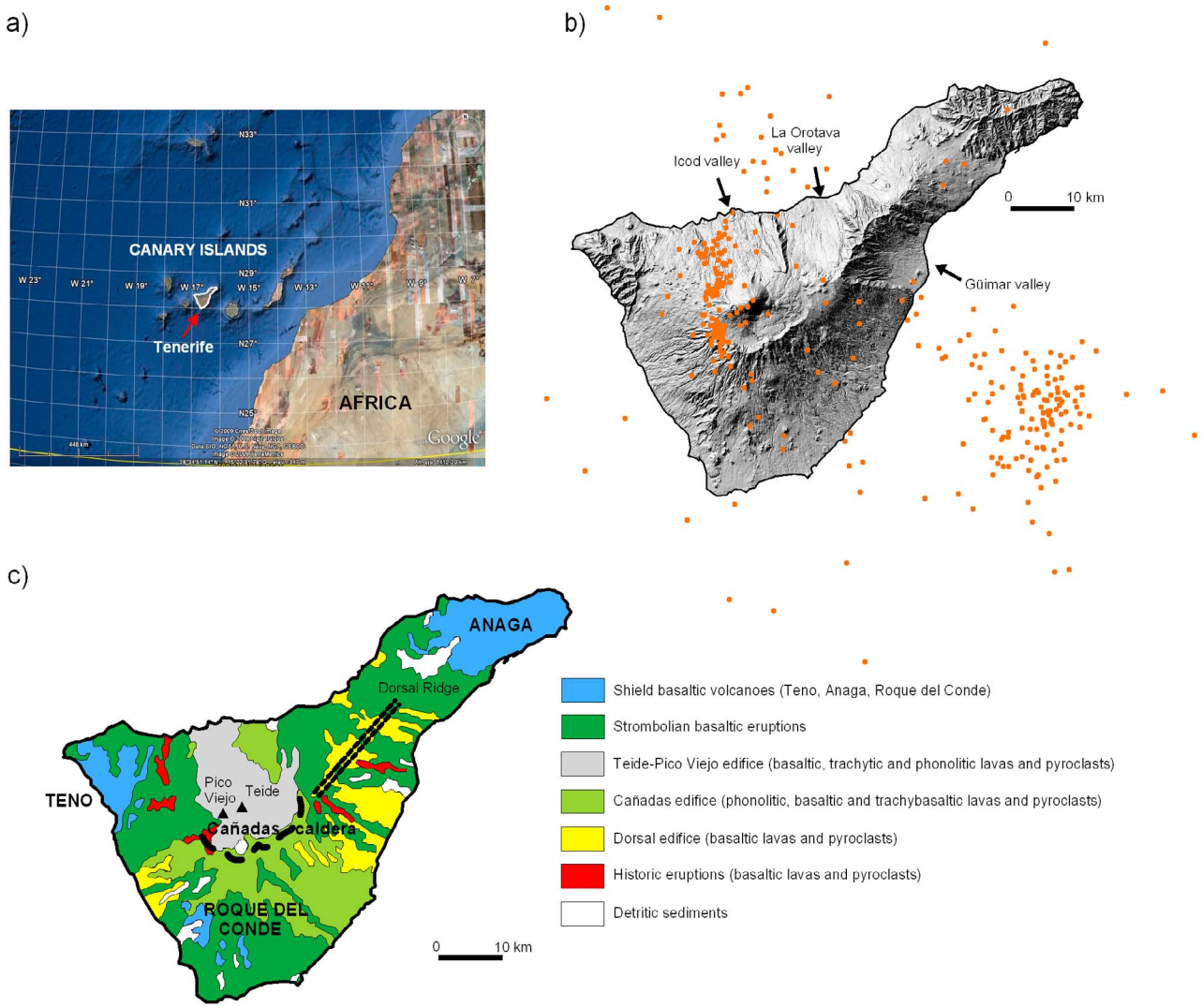

Figure 1. (a) Geographic location of the Canary Islands; (b) shaded topography of Tenerife and location of the epicenters of the seismic activity recorded in Tenerife and its surrounding marine area during 2004 and 2005 (data from the Spanish Instituto Geográfico Nacional available at http://www.ign.es); (c) simplified geological map of Tenerife [see *Instituto Geológico y Minero de España*, 2004].

that rift zones are due to the gravitational spreading of the volcanic edifice over a deformable substratum and therefore develop in a later stage of growth of the island, when the island reaches such a volume that makes it unstable [e.g., *Münn et al.*, 2006]. In the case of Tenerife, both theories have been proposed and the presence of a triaxial rift system itself has been questioned [*Carracedo*, 1994; *Martí et al.*, 1996; *Walter*, 2003; *Geyer and Martí*, 2010].

[5] Rift zones are frequently prone to collapse. Recent studies show that they represent geologically unstable structures that migrate and reorganize in response to volcano flank instability, although it remains unclear whether rifting is a cause or a consequence of flank deformation [*Walter and Troll*, 2003; *Walter et al.*, 2005]. In the Canary Islands, investigations into these issues are quite recent, and the importance of giant collapses as major destructive events of the volcanic edifices has become evident only in the last few years [*Watts and Masson*, 1995; *Teide Group*, 1997; *Ancochea et al.*, 1999; *Cantagrel et al.*, 1999; *Hürlimann et al.*, 1999; *Ablay and Hürlimann*, 2000; *Watts and Masson*, 2001; *Walter and Schmincke*, 2002].

[6] Rift zone identification is usually only based on surface evidence, such as concentration and alignment of volcanic vents, dike orientation, location of topographic ridges, etc. However, this approach based on surface evidence alone can lead to an incomplete description of ocean island volcanoes since it ignores most of the volume of the volcanic edifice. Geophysical methods, particularly studies of potential fields, can supply additional constraints for a more complete model of the structure of volcanic islands. Aeromagnetic data have the great advantage of providing a high-quality magnetic image based on homogeneously distributed measurements acquired in a short period of time. In addition, volcanic rocks contain significant quantities of magnetic minerals, especially magnetite. For this reason, volcanic areas are usually characterized by a strong magnetic

signal. When airborne magnetic data are measured at heights ranging from several hundred meters to one or more kilometers from the surface, the observed magnetic anomalies are mostly due to intrusive bodies with an important vertical extent. Thus, this kind of data is especially useful for imaging mafic cores, intrusive complexes, dike swarms, etc. Therefore, aeromagnetic data can help reveal the deep structure and the feeding system of ocean island volcanoes, contributing to a better understanding of their rift zones. This type of study has already been applied to the island of El Hierro [*Blanco-Montenegro et al.*, 2008]. Magnetic anomalies of some other islands of the Canary archipelago have also been investigated, such as Gran Canaria [*Blanco-Montenegro et al.*, 2003] and Lanzarote [*Blanco-Montenegro et al.*, 2005]. These studies were based on aeromagnetic data acquired in a survey of the Canary Archipelago carried out in 1993 by the Spanish National Geographic Institute (IGN) [*Socías and Mézcua*, 1996]. The IGN aeromagnetic data were also used to construct simple 2.5D models of the inner structure of the central part of the island of Tenerife [*Araña et al.*, 2000].

[7] In 2006, a new aeromagnetic survey of Tenerife was carried out with the aim of sampling the magnetic signature of the island with unprecedented detail [*García et al.*, 2007]. In this work, we present 3-D magnetic models of Tenerife obtained from this new data set through an inverse approach specifically adapted to the characteristics of volcanic environments. These models cast new light on the inner structure of this volcanic island and help answer some of the open questions about the evolution of ocean island volcanoes.

2. Geological Setting

[8] Tenerife is the largest of the Canary Islands and is located in the central part of the archipelago (Figure 1a). Although about 90% of the total volume of ocean islands corresponds to their submarine portion [*Schmincke*, 2004], very little information is usually available about the seamount stage of growth. This also applies to the case of Tenerife, where our geological knowledge is restricted to the subaerial part of the volcanic edifice. This part of the edifice has a volcanic history that spans about 12 Ma. The first paper presenting a comprehensive reconstruction of the volcanic evolution of Tenerife based on radiometric age determinations was published by *Ancochea et al.* [1990]. Recently, new geochronologic and paleomagnetic data have allowed a more precise definition of the timing of the subaerial stages of growth of the island [*Thirlwall et al.*, 2000; *Huertas et al.*, 2002; *Guillou et al.*, 2004; *Leonhardt and Soffel*, 2006; *Carracedo et al.*, 2007; *Carracedo et al.*, 2009]. The following description reports these new data.

2.1. Initial Stages in the Volcanic Evolution of Tenerife

[9] Three deeply eroded, old massifs (Anaga, Teno, and Roque del Conde, also known as Central shield; see Figure 1c) represent the remnants of the shield-building phase, which is generally thought to be the most important phase of subaerial growth of an ocean island. The Central shield was formed between 11.9 and 8.9 Ma and is represented by the outcrop of Roque del Conde, in the SW of the island. The Teno massif, in the NW, erupted between 6.3 and 5.3 Ma, whereas the Anaga massif was formed in the NE of the island between 4.9 and 3.9 Ma. These massifs are made up of accumulations of predominantly basaltic rocks culminated with felsic materials, and are generally known as Old Basaltic Series. This nomenclature has been used since the first volcanological studies of Tenerife [*Fúster et al.*, 1968].

[10] After the formation of the three basaltic shield volcanoes, the volcanic activity was concentrated in two large edifices: the Cañadas composite volcano, in the central part of the island, and the Dorsal edifice, a SW-NE ridge linking the Cañadas edifice and the Anaga massif. In the Cañadas edifice, the activity extended for more than 3.5 Ma in several phases of intense volcanic activity separated by phases of erosive destruction and flank failure. This central volcano edifice is considered to have grown up to 3000 m above sea level with a radius of approximately 17 km, and was made up of basalts, trachybasalts, trachytes and phonolites [*Martí et al.*, 1994; *Ancochea et al.*, 1999; *Huertas et al.*, 2002]. The Dorsal edifice, also known as Pedro Gil, was formed by basaltic eruptions that started around 1.0 Ma ago and continued up to the present time [*Ancochea et al.*, 1990, 1999].

2.2. The Cañadas Caldera and the Teide-Pico Viejo Complex

[11] On the upper part of the Cañadas edifice, in the center of Tenerife, there is a large depression known as the Cañadas caldera (see Figures 1b and 1c). This depression has an elliptical shape, measuring 16 km along its longest axis, and is partially surrounded by a wall up to 500 m high in its southern and eastern sectors. The origin of this caldera is still a matter of intense debate. Some authors related the formation of the Cañadas caldera to the occurrence of repeated flank failure [e.g., *Carracedo*, 1994; *Watts and Masson*, 1995; *Ancochea et al.*, 1999; *Cantagrel et al.*, 1999], whereas others consider that it is the result of vertical collapses related to explosive activity and the migration of the associated magma chamber [e.g., *Ablay and Hürlimann*, 2000; *Martí and Gudmundsson*, 2000; *Brown and Branney*, 2004]. The coincidence in time of the most recent giant landslides and caldera-forming events has led some authors to suggest that seismicity associated with vertical collapses may have triggered major landslide events [*Martí et al.*, 1997; *Hürlimann et al.*, 1999]. Two recent geophysical investigations, one based on audiomagnetotelluric soundings [*Coppo et al.*, 2008] and the other based on gravity data [*Gottsmann et al.*, 2008], support the vertical collapses hypothesis.

[12] The most recent phase of activity in Tenerife involved the formation of the Teide-Pico Viejo complex inside the northern part of the Cañadas caldera, with the Teide peak emerging as the highest point of the island. Teide and Pico Viejo are two twin stratovolcanoes of basanitic-phonolitic composition. Their formation spans between 200 ka and the present time [*Ablay and Martí*, 2000; *Carracedo et al.*, 2007]. In addition, recent volcanic activity is responsible for a large number of monogenetic volcanoes throughout the island. In the last 300 years, six eruptions have taken place in Tenerife. The last event, the Chinyero eruption, occurred in 1909 in the northwestern flank of the Teide edifice [e.g., *Dóniz et al.*, 2008].

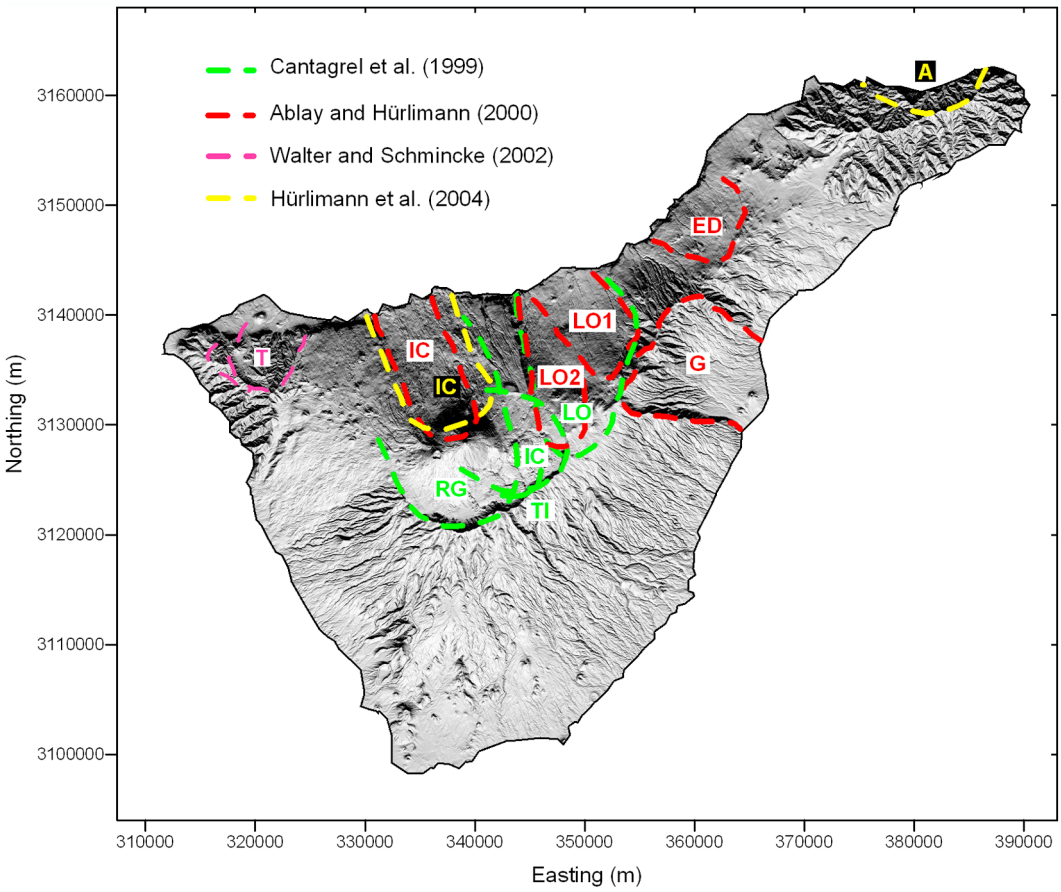

Figure 2. Location of the headwalls of flank collapses in Tenerife proposed by different authors (T, Teno; A, Anaga; IC, Icod; LO, La Orotava; RG, Roques de García; TI, Tigaiga; G, Güímar; ED, East Dorsal).

2.3. Giant Landslides

[13] One of the most important mechanisms of mature volcano dismantling is flank failure, capable of removing several hundreds of cubic kilometers almost instantly. The discovery of events of this kind is relatively recent in the Canaries and, specifically, in Tenerife. Although some geological studies suggested that some collapses may have affected the north flank of the island [*Bravo*, 1962; *Coello*, 1973], the first evidence arrived in the 1990s, when high-resolution bathymetry data revealed the presence of voluminous debris avalanche deposits off the north coast [*Watts and Masson*, 1995; *Teide Group*, 1997]. At least six giant landslides of the north and northeast flanks of Tenerife have been identified, although the number of events and the location of the corresponding scars is subject to debate, especially in the central part of the island (see Figure 2) [*Ancochea et al.*, 1999; *Cantagrel et al.*, 1999; *Hürlimann et al.*, 1999; *Ablay and Hürlimann*, 2000; *Watts and Masson*, 2001; *Walter and Schmincke*, 2002].

[14] The oldest events involved the shield basaltic edifices of Anaga and Teno. The former was affected by one flank failure of unknown age, whereas the latter collapsed twice at about 6 Ma ago [*Cantagrel et al.*, 1999; *Walter and Schmincke*, 2002].

[15] The La Orotava valley is commonly considered to have originated from landsliding. However, whereas some authors explain its formation with a single event between 690 ka and 540 ka [*Cantagrel et al.*, 1999; *Masson et al.*, 2002], other propose the occurrence of two separate collapses between 730 ka and 560 ka [*Ablay and Hürlimann*, 2000; *Hürlimann et al.*, 2004] (see Figure 2). The formation of the present Icod valley, located to the west of La Orotava, is much more controversial, especially regarding the location of the headwall of the originating collapse, which has been dated between 1.20 and 0.17 Ma [*Watts and Masson*, 1995]. *Cantagrel et al.* [1999] placed the scar of the collapse in correspondence with the southeast Cañadas caldera wall, thus explaining the formation of this part of the caldera with landsliding. They also proposed the occurrence of another two collapses in this area: the Roques de García event, responsible for the origin of the western part of the Cañadas caldera, and the Tigaiga landslide (see Figure 2). The occurrence of the Roques de García landslide has been questioned by *Ablay and Hürlimann* [2000] and *Hürlimann et al.* [2004], who considered that only one collapse took place in the area of the Icod valley, with its headwall located somewhere beneath the northern slopes of the Teide and Pico Viejo stratovolcanoes.

[16] Two other landslides have been identified in Tenerife, both involving the flanks of the Dorsal edifice (Figure 2): the East Dorsal collapse, of unknown age [*Ablay and Hürlimann*, 2000]; and the Güímar collapse, which has been dated at 780 to 830 ka [*Ancochea et al.*, 1990; *Cantagrel et al.*, 1999; *Masson et al.*, 2002].

2.4. Rift Zones

[17] The identification and study of rift zones in Tenerife has become an issue of interest for volcanologists in recent years. *Carracedo* [1994] stated that a convergent three-armed rift exists in Tenerife with axes following NW-SE, NE-SW and N-S directions. He proposes that this rift system controlled the occurrence of volcanic activity from the basaltic shield stage to the present time. Carracedo based his interpretation on eruptive vent concentration and dike density observed in tunnels excavated while searching for water. However, the three-armed rift model and, specifically, the existence of its N-S branch has been questioned by *Martí et al.* [1996] and *Geyer and Martí* [2010], who pointed out that the NW-SE and ENE-WSW trends can be identified all throughout the island, including the southern portion of the island where the N-S rift arm is supposed to be. This suggests that long-lived regional tectonics have controlled the distribution of volcanism. Recent eruptive vents in the southern half of Tenerife seem too scattered to define an alignment [*Ancochea et al.*, 1995; *Hürlimann et al.*, 2004].

[18] Regarding the origin of rift zones in Tenerife, *Carracedo* [1994] proposed that they formed due to magma-induced updoming of the lithosphere, which produced a least-effort fracture configuration with typical separation angles of 120°. This mechanism implies that rift zones are deeply rooted beneath the volcano and were initiated early in the island's history. Analogue experiments, however, suggested that the triaxial structure of Tenerife is related mainly to volcano spreading. Therefore, this rift skeleton was not present during the early phases of growth of the island, but appeared later in the evolution of the volcanic edifice when it became gravitationally unstable [*Walter*, 2003].

3. Magnetic Data

[19] The magnetic data used in this work were acquired in April-May 2006 in the framework of a research project aimed at imaging the inner structure of Tenerife. This project involved Spanish (Consejo Superior de Investigaciones Científicas and Universidad de Burgos) and Italian (Istituto Nazionale di Geofisica e Vulcanologia) institutions. Almost 5000 km of aeromagnetic profiles were flown with a helicopter, with main N-S lines spaced at 1000 m in the central and the eastern parts of the island and at 2000 m in the rest of the survey area, which also included the submarine portion of the volcanic edifice. Tie lines were flown E-W and spaced 5000 m apart. Over the highest part of the island (the Cañadas caldera and the Teide-Pico Viejo complex), magnetic data were measured using draped profiles, maintaining a terrain clearance of about 150 m. Outside of this central area, the flight height was 2200 m. A detailed explanation of the survey parameters and of the data processing is described by *García et al.* [2007]. The final magnetic anomaly map of Tenerife is shown in Figure 3. For this work, we subsampled the high-resolution grid with a new cell size of 1700 m in the north-south and east-west directions.

4. Analysis of the Magnetic Anomalies

4.1. Removal of Long-Wavelength Components From the Magnetic Data Set

[20] The magnetic anomaly map of Tenerife contains a long-wavelength magnetic component that had to be removed from the data prior to the modeling. The identification and removal of this component from the data set were not obvious, since after the application of typical detrending procedures, the magnetic anomaly map of Tenerife still contained a long-wavelength component that significantly warped the magnetic pattern from the zero level.

[21] We chose to approach this problem through Fourier analysis. We used the magnetic data set of the entire Canary archipelago, measured in 1993 [*Socías and Mézcua*, 1996]. This data set represented regional components better than the 2006 anomaly map, which only covers the island of Tenerife. In fact, we verified that a high-pass filtering of the 2006 data set did not remove the long-wavelength component properly. Therefore, we filtered the magnetic map of the Canary Islands measured in 1993 using different cutoff wavelengths and studied both the resulting low-frequency (usually linked to more regional features) and high-frequency (related to the volcanic edifice) magnetic anomaly maps in the area of Tenerife. We found that a cutoff wavelength of 75 km was suitable since with this value the most important anomalies of the island were adequately leveled around the zero value while their shape remained almost unchanged. Moreover, 75 km is roughly the diameter of the island. From the geological point of view, the long-wavelength filtered component is likely to be related to the magnetic signal of the Jurassic oceanic crust and with the longest-wavelength magnetic signal of the volcanic edifice.

[22] In order to obtain a magnetic map where anomalies were only related with sources located within the volcanic edifice, we subtracted the low-pass-filtered anomaly obtained from the 1993 regional survey (Figure 4a) from the 2006 data set of Tenerife. This subtraction is valid because the difference in acquisition height between both data sets is negligible for the range of wavelengths involved. The final magnetic anomaly map of Tenerife used in this work is shown in Figure 4b.

4.2. Estimation of the Direction of the Total Magnetization Vector

[23] In volcanic areas, the natural remanent magnetization (NRM), mainly of thermoremanent origin, is by far the most important component of the total magnetization vector. This means that the direction of the magnetization is an unknown to be determined prior to the magnetic anomaly modeling, since it can be significantly different from the ambient magnetic field direction. Generally, a constant magnetization direction is assumed to characterize all the geological structures of the studied area.

[24] We have applied the method proposed by *Nicolosi et al.* [2006] to estimate the direction of the total magnetization vector in the case of Tenerife. This method is based on an equivalent source inversion approach, and consists of

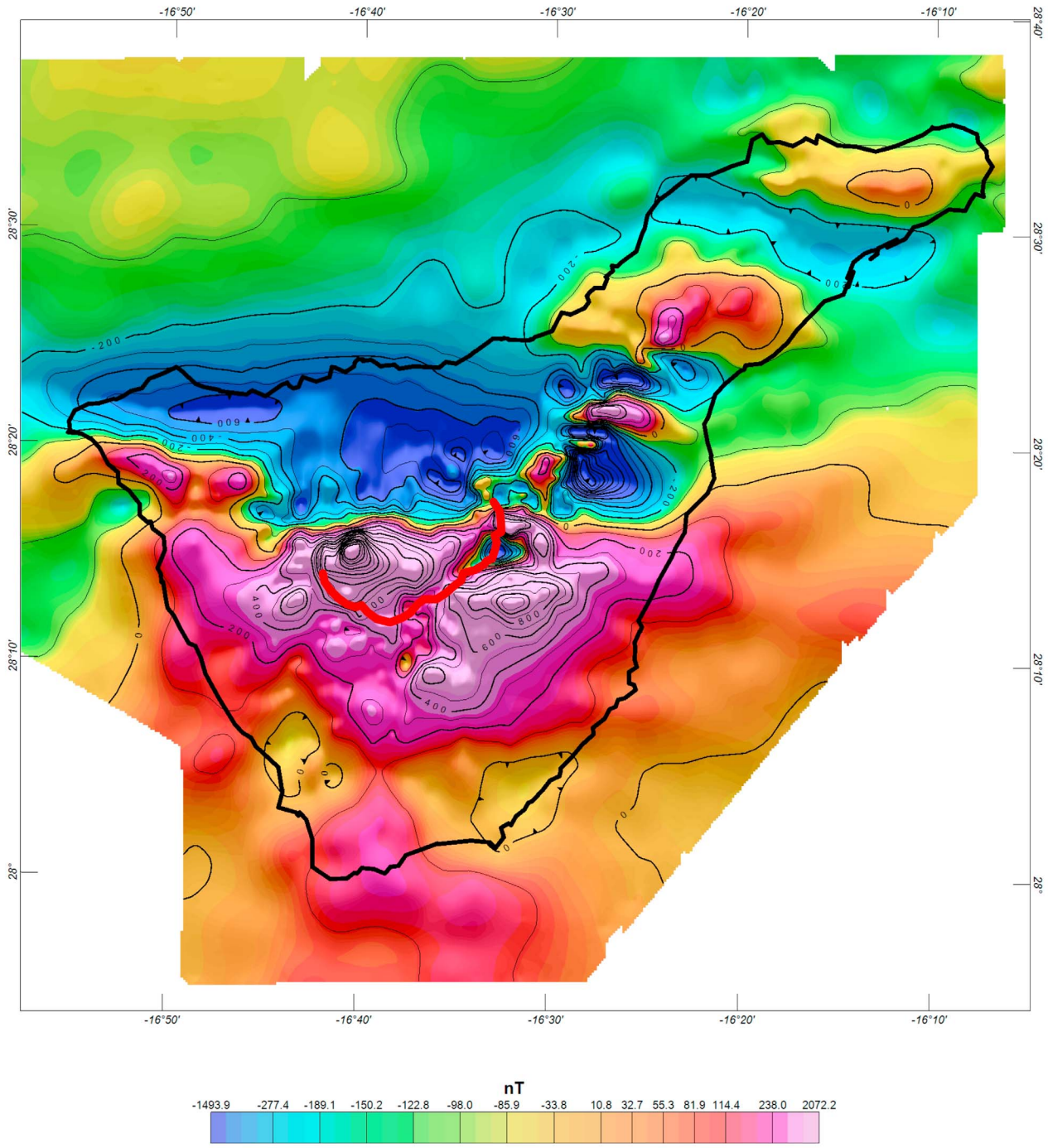

Figure 3. High-resolution magnetic anomaly map of Tenerife. The cell size of this grid is 250 m both in the east-west and north-south directions. For details, see *García et al.* [2007]. The thick red line shows the location of the Cañadas caldera wall.

obtaining a magnetization distribution in one flat layer for different pairs of values of inclination (I) and declination (D) of the magnetization. The source layer is discretized into a number of prismatic cells and the magnetization of each cell is found by linear inversion. Each inversion produces a magnetic model that can reproduce the observed magnetic anomaly. The accuracy of the magnetic field produced by each model (that is, for a given I and D), as compared to the actual magnetic anomaly data, can be quantified by calculating the misfit between both data sets (χ^2). In synthetic tests, the best fit always corresponds to the pair (I, D) that is closest to the actual direction of the total magnetization vector. Therefore, if an inversion model is calculated for different pairs (I, D) from a selected range of values, and the misfit between the magnetic field of each model and the actual magnetic anomaly is calculated, then the total magnetization vector can be estimated as the pair (I, D) that corresponds to the lowest value of χ^2.

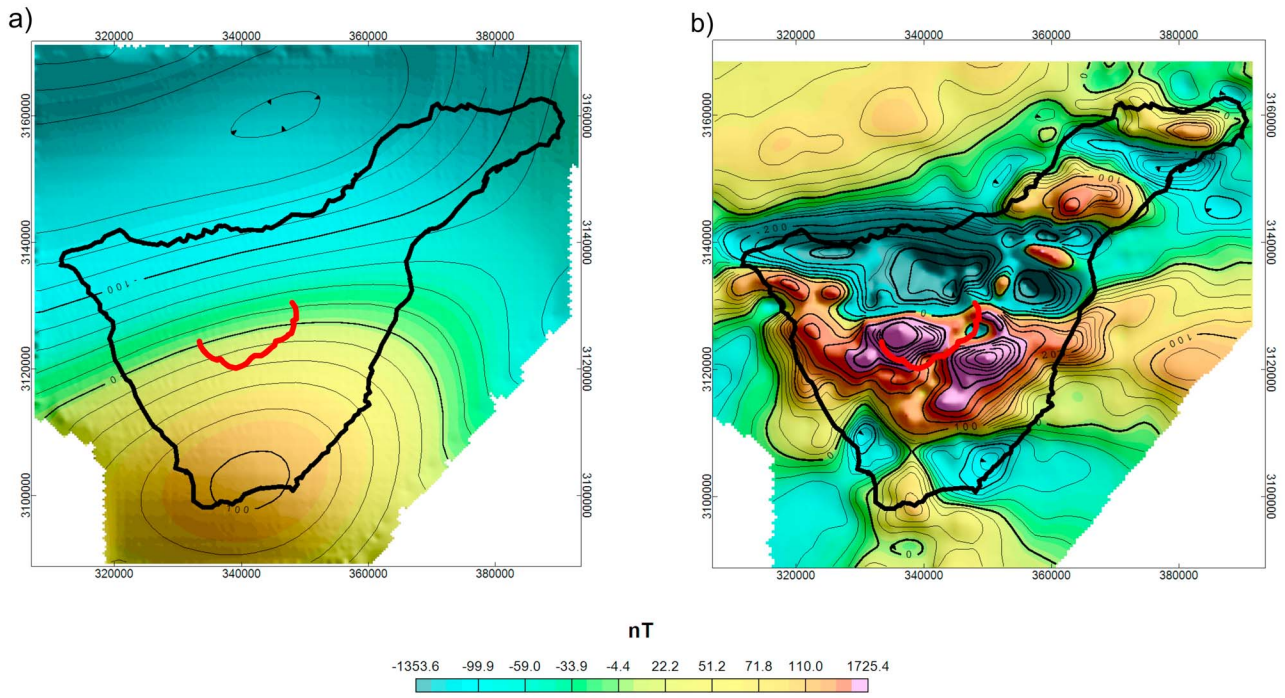

Figure 4. (a) Long-wavelength component of the magnetic anomalies of Tenerife obtained from the regional aeromagnetic data set of the Canary Islands measured in 1993 (see text for details); (b) residual magnetic anomaly field of Tenerife obtained by subsampling the magnetic anomaly grid shown in Figure 3 and removing the magnetic field of Figure 4a. The cell size of this grid is 1700 m both in the east-west and north-south directions. The thick red line shows the location of the Cañadas caldera wall.

[25] We have applied this method to the residual magnetic anomaly of Tenerife as illustrated in Figure 4b, where the long-wavelength magnetic components that are unrelated to the volcanic edifice have been removed. The top of the source layer, 3 km thick, was located at the sea level, and it was divided into prismatic cells measuring 3 km × 3 km in the N-S and E-W directions. The magnetic field direction was modeled with the 10th generation of the International Geomagnetic Reference Field (IGRF) [*MacMillan and Maus*, 2005] in Tenerife at the epoch of the survey (2006.3), which gives an inclination $I = 38°$ and a declination $D = -7°$. By inverting the residual magnetic anomaly of Tenerife, we obtained a magnetization distribution on the source layer for 315 pairs of values (I, D), where I and D were within the range from 10° to 80° and −50° to 50°, respectively, at intervals of 5°. The model that best fits the actual data (lowest χ^2) corresponds to the magnetization direction $I = 50°$, $D = 0°$ (see Figure 5). This result agrees very well with the direction of the axial dipole field in Tenerife ($I = 47°$, $D = 0°$), suggesting that the main component of the bulk magnetization of the volcanic edifice is a remanence acquired during a time span of several million years.

[26] A reduced-to-the-pole anomaly map of Tenerife based on the magnetic anomalies shown in Figure 4b is provided in the auxiliary material for the interested reader (Figure S1).[1] This kind of transformation converts an

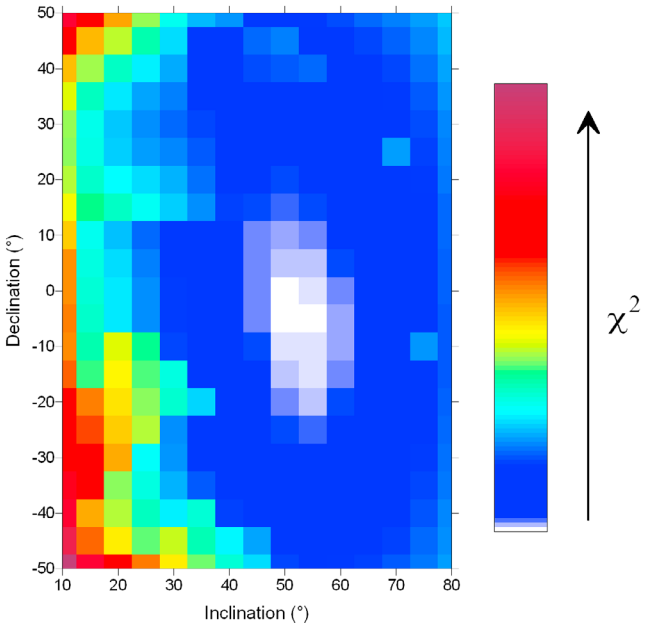

Figure 5. Misfit between actual and synthetic magnetic anomaly data obtained through linear inversion on a flat layer for different magnetization directions. The best fit (lowest χ^2) reveals the actual magnetization direction, defined by an inclination $I = 50°$ and a declination $D = 0°$.

[1] Auxiliary materials are available in the HTML. doi:10.1029/2010JB007646.

anomaly map in the one that would be observed at the magnetic pole, where the magnetic field is vertical and the resulting anomalies are not dipolar. Reduction to the pole was carried out considering that the magnetization direction is given by the declination and inclination values obtained through the method previously described ($I = 50°$, $D = 0°$). The ambient magnetic field was modeled with the IGRF, as we pointed out before ($I = 38°$, $D = -7°$).

5. Inversion of Magnetic Data

[27] The main purpose of studying the aeromagnetic anomalies of Tenerife was to obtain a 3-D model of the inner structure of the island using magnetic inversion algorithms. Once the magnetization direction was calculated from the data, the next step of our interpretation strategy was to obtain a distribution of the length of this vector inside the island volume.

[28] Magnetic inversion is limited by the nonuniqueness inherent to potential fields and by algebraic ambiguity, which implies that an infinite number of magnetization distributions can reproduce the observed magnetic anomalies [*Blakely*, 1995]. The usual approach to solve the inverse problem involves reducing the number of degrees of freedom by introducing constraints about the source parameters and applying numerical techniques, such as optimization algorithms. Therefore, each inversion approach defines a priori which kind of model will be obtained.

[29] In this work, we used two inversion methods: one of them aimed at finding lateral magnetic contrasts and identifying correlations between the magnetization distribution and previously known volcanic and volcano-tectonic features (linear inversion), and the other aimed at imaging the deep intrusive structures of Tenerife (nonlinear inversion).

5.1. Linear Magnetic Inversion

[30] Let us consider a continuous distribution of magnetization $J(r)$ inside a source volume V, with a constant direction given by the unit vector $\mathbf{t}$. The magnetic anomaly ΔT measured at the position $\mathbf{r'}$ outside the volume V is given by

$$\Delta T(\mathbf{r}') = \frac{\partial^2}{\partial \mathbf{f}\, \partial \mathbf{t}} \int_V \frac{J(\mathbf{r})}{|\mathbf{r} - \mathbf{r}'|}\, dv, \tag{1}$$

where $\mathbf{f}$ is the unit vector along the ambient magnetic field direction. If the source volume is divided into a set of N homogeneous prismatic subvolumes and the magnetic anomaly is measured at a discrete set of M points, then equation (1) can be rewritten as

$$\Delta T_m = \sum_{i=1}^{N} G_{i,m} J(\mathbf{r}_i) \quad m = 1,\ M, \tag{2}$$

where

$$G_{i,m} = \frac{\partial^2}{\partial \mathbf{f}\, \partial \mathbf{t}} \int_V \frac{1}{|\mathbf{r}_i - \mathbf{r}_m|}\, dv,$$

where $J(\mathbf{r}_i)$ is the magnetization of subvolume V_i and ΔT_m is the magnetic anomaly measured at station m. The kernel $G_{i,\,m}$ represents the magnetic anomaly at station m due to the subvolume V_i with unit magnetization along direction $\mathbf{t}$.

[31] In matrix form, equation (2) becomes

$$\mathbf{T} = \hat{G}\mathbf{J}, \tag{3}$$

where $\mathbf{T}$ is the M vector of magnetic data, $\mathbf{J}$ is the N vector of magnetizations and $\hat{G}$ is the $M \times N$ kernel with elements that were determined using the magnetic effect for the rectangular prism from *Sharma* [1986].

[32] The estimation of the source magnetization, $\mathbf{J}$, can be achieved by solving the linear system reported in equation (3). In general, systems of this kind are underdetermined and their solution must be found by means of numerical techniques [*Jackson*, 1972; *Press et al.*, 1992]. To solve this linear system, we adopted the Levenberg-Marquardt iterative regularization minimization method [*Press et al.*, 1992], simultaneously minimizing the norm of the solution and the misfit between the observed and the computed synthetic magnetic anomalies generated by the magnetization solution vector [*Bear et al.*, 1995].

[33] To apply the linear inversion method to the magnetic anomalies of Tenerife, we considered a source volume defined by a top surface coinciding with the topography of the island and a flat bottom surface corresponding to the seafloor in the vicinity of Tenerife. This volume was divided into a number of vertical prismatic cells, measuring 2 km × 2 km in the N-S and E-W directions, where the thickness of each prism was given by the topographic height at the center of the prism measured from the seafloor depth, which was estimated in 4 km below sea level. We assumed that all prisms were magnetized along the direction obtained in section 4.2 ($I = 50°$, $D = 0°$). For the magnetic field, we used the direction given by the IGRF at the epoch of the survey ($I = 38°$, $D = -7°$) [*MacMillan and Maus*, 2005].

[34] This kind of magnetic inversion produces a magnetization value for each cell that represents an average value for the whole prism volume, from its top to its bottom (Figure 6). This means that this approach neglects horizontal magnetization contrasts that can be present within individual prisms. The use of a two-dimensional magnetization distribution has the advantage of considerably reducing the number of degrees of freedom of the system. This approach is especially useful for revealing lateral magnetic contacts, which can be related to intrusive structures and the feeding system of the volcanic edifice.

[35] In section 6 we analyze the coherence between the magnetic model shown in Figure 6 and surface magnetic polarities measured in the field by *Carracedo* [1979] (Figure 7).

5.2. Nonlinear Magnetic Inversion: Constant Magnetization Model

[36] We attempted to image the inner structure of Tenerife Island by means of constant magnetization models. The purpose of this analysis was to highlight the geometry of the main magnetic source of Tenerife in the assumption that the internal magnetization variation of this body is not relevant. The body we wanted to image represents intrusive complexes and feeding systems beneath central Tenerife. It is important to note that the magnetic effect of these structures can be realistically modeled using a bulk magnetization

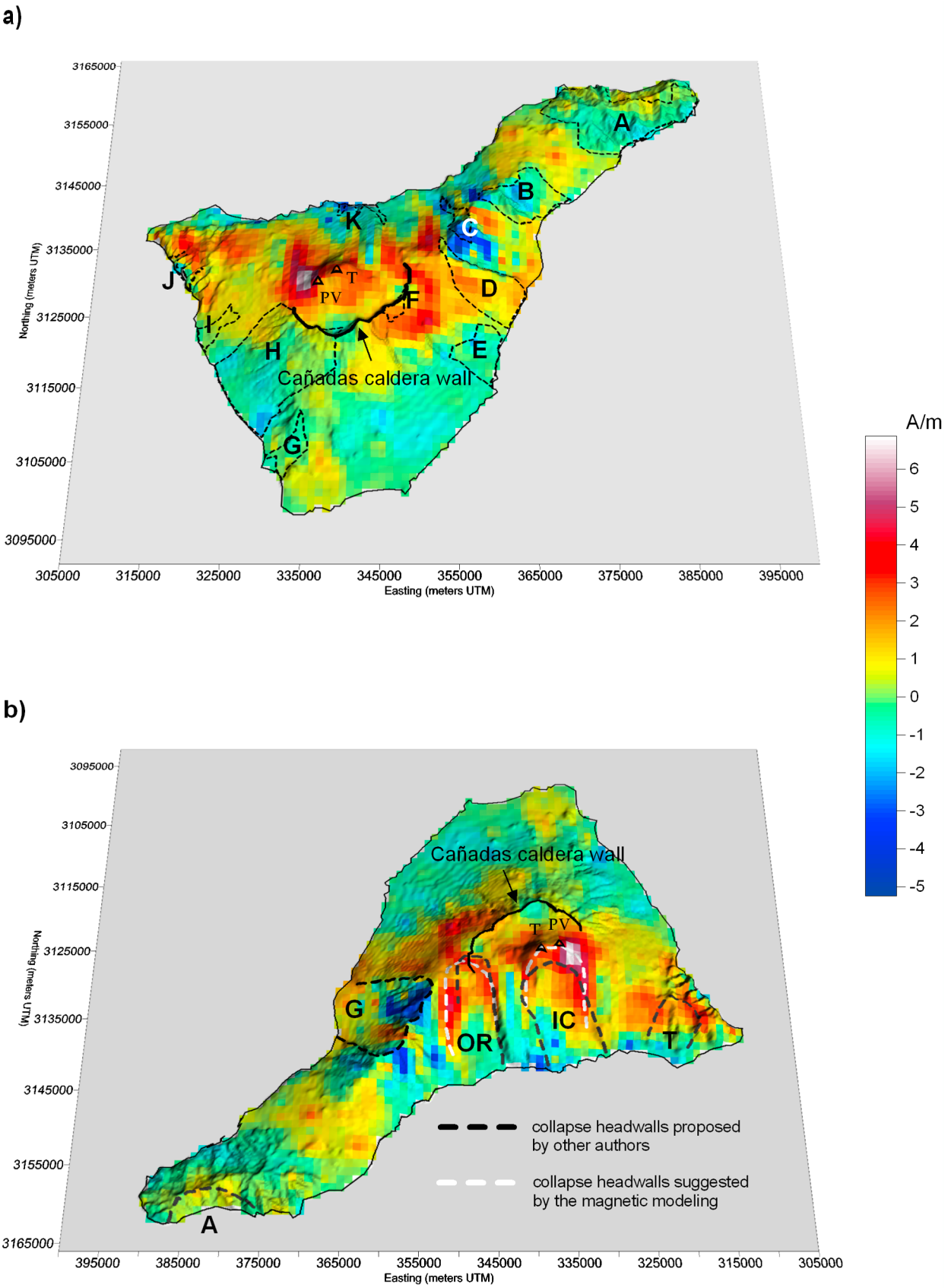
a)
A
B
C
D
E
F
G
H
I
J
K
T
PV
Cañadas caldera wall
Northing (meters UTM)
Easting (meters UTM)
3165000
3155000
3145000
3135000
3125000
3115000
3105000
3095000
305000
315000
325000
335000
345000
355000
365000
375000
385000
395000
A/m
6
5
4
3
2
1
0
-1
-2
-3
-4
-5
b)
Cañadas caldera wall
T
PV
G
OR
IC
T
A
collapse headwalls proposed by other authors
collapse headwalls suggested by the magnetic modeling

Figure 6

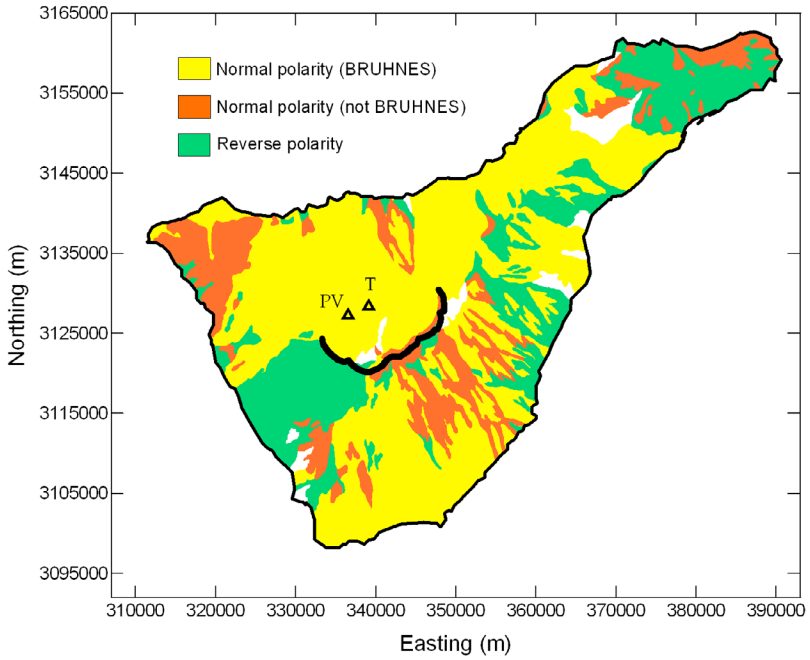

Figure 7. Surface magnetic polarity map of Tenerife [see *Carracedo*, 1979]. The thick black line shows the location of the Cañadas caldera wall. The small black triangles show the location of the Pico Viejo (PV) and Teide (T) craters.

value. This model is realistic in spite of the structural complexity (highly magnetized dike swarms intruded into volcanic materials) because we measured the magnetic field at a distance of the order of several kilometers from the source.

[37] To build this kind of model, we set a reference magnetization value that each cell can assume, instead of starting at zero. The model was obtained using a nonlinear iterative inversion approach. We used the simplex search strategy [*Lagarias et al.*, 1998], which is a direct search method that does not use numerical or analytic gradients. Starting from equation (3), we defined the minimization of an objective function as:

$$\min_{x\in\Re} (\mathbf{T} - \hat{G}\mathbf{J}(x)), \tag{4}$$

where the vector **J**(x) is a function defined as:

$$\begin{aligned} \mathbf{J}(\mathrm{x}) &= 0 \text{ if } \mathrm{x} < 0 \\ \mathbf{J}(\mathrm{x}) &= j \text{ if } \mathrm{x} \geq 0, \end{aligned} \tag{5}$$

and j is the constant magnetization value of the model.

[38] We expressed the magnetization vector **J** as a function of an independent variable $x \in \Re$ so that the set of x values found by the minimization process plays the role of "turning on" or "off" the cells. This approach has the advantage of generating model solutions that do not depend on mathematical optimization forms, such as the minimization of L1, L2 or the Euclidean norm. At the same time, it has the disadvantage of decreasing the fitting quality.

[39] We built a 3-D mesh of blocks, each of them measuring 3000 × 3000 × 1000 m along the easting, northing and vertical directions, respectively. This source volume ranged from 3000 m above sea level to 10000 m below sea level. We used 5590 cells, centering the mesh on the geometrical center of Tenerife, corresponding to 347,815 m east, 3,129,282 m north in the UTM projection (zone 28N). We calculated four different inversion models using 2, 3, 4, and 6 A m^{-1} for the magnetization, with constant inclination and declination of 50° and 0° and inclination and declination of the main field of 38° and −7°, respectively. The four magnetization values represent a reasonable range to explore how sensitive the recovered model is to different magnetizations. The four models thus obtained are very similar. The main differences between them are related to the depth to the bottom of the sources: low magnetization values imply much thicker bodies. In Figures 8 and 9, the model obtained using a constant magnetization of 3 A m^{-1} is shown. This is

Figure 6. Two different perspectives of the magnetization distribution obtained through linear inversion of the magnetic anomaly map of Tenerife shown in Figure 4b: (a) polygons represent the areas characterized by a surface paleomagnetic reverse polarity (see Figure 7); (b) dashed lines show the location of the headwalls of the Icod (IC), La Orotava (OR), Güímar (G), Teno (T) and Anaga (A) landslides (see Figure 2). The small black triangles show the location of the Pico Viejo (PV) and Teide (T) craters.

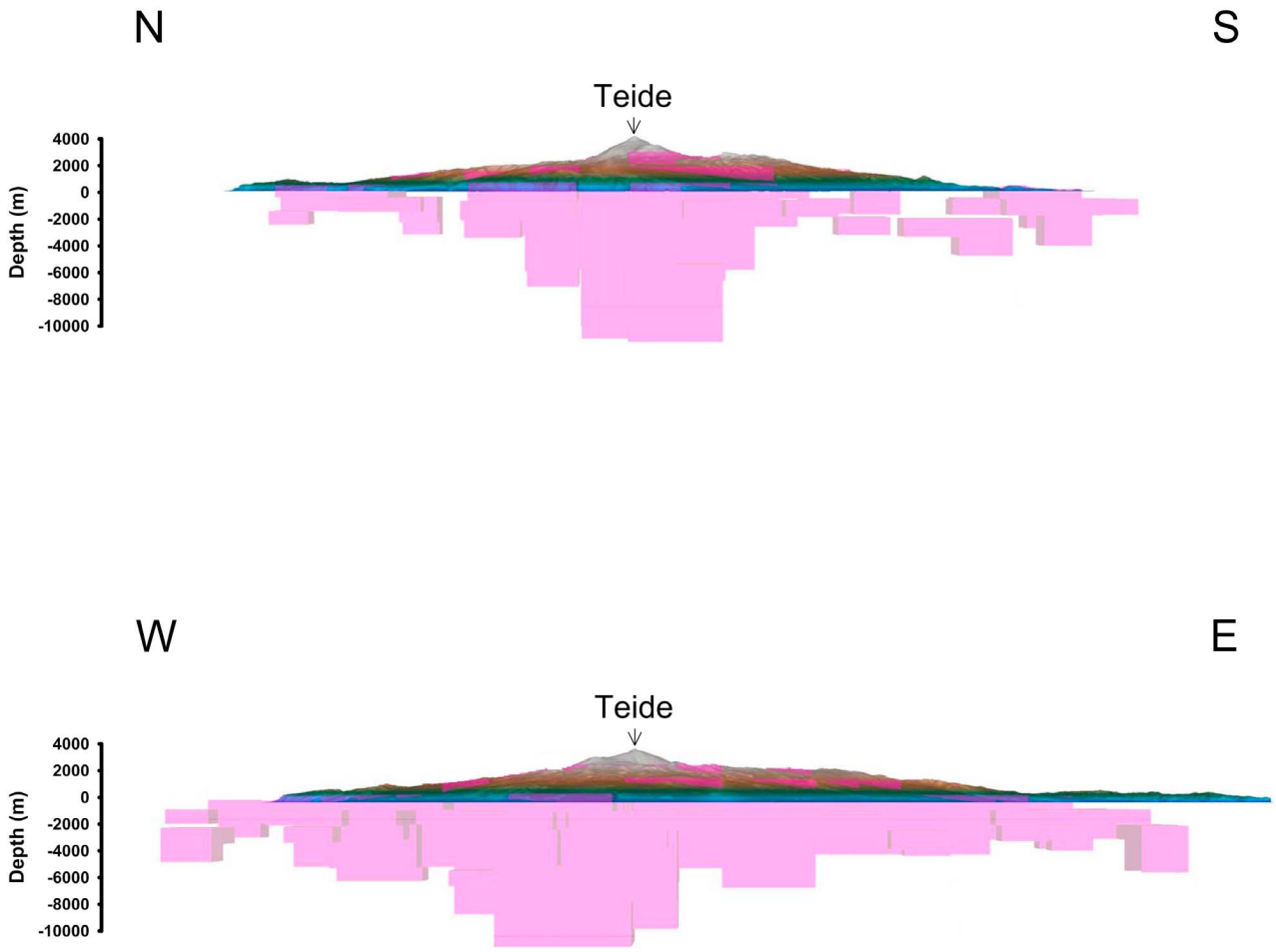

Figure 8. A 3-D magnetic model of Tenerife obtained through nonlinear inversion of the magnetic data shown in Figure 4b, assuming a constant magnetization value for the main sources of 3 A m^{-1}: view of the model (top) from the east and (bottom) from the south. Note the shading of the blocks, which indicates that these are not vertical sections but two perspective views of the whole structure.

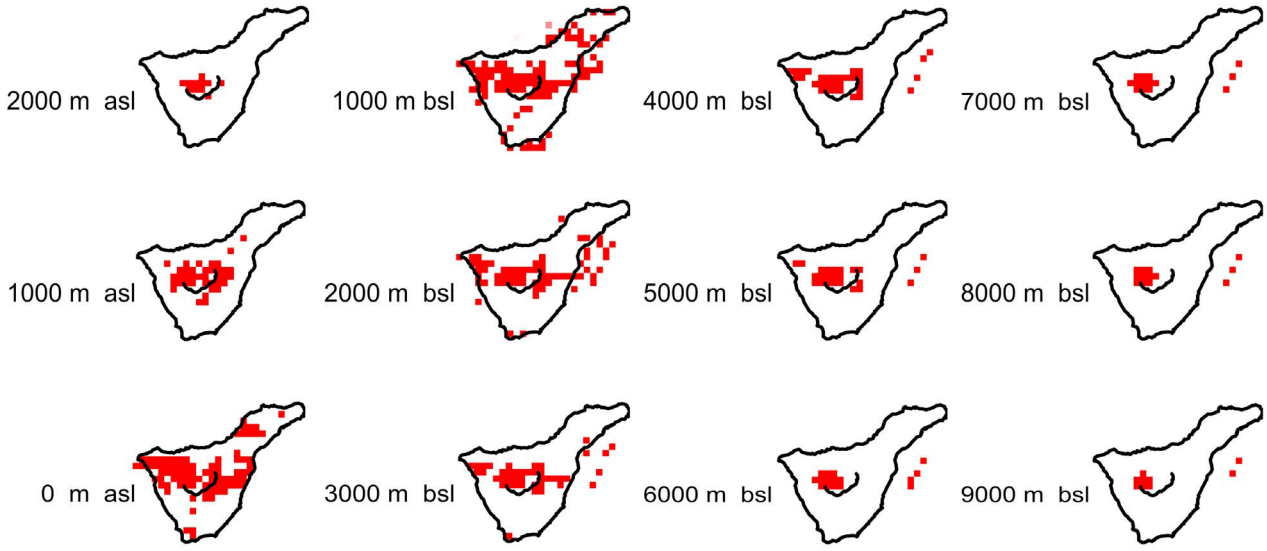

Figure 9. Horizontal slices of the model shown in Figure 8 at different depths above (asl) and below (bsl) the sea level. The black line in the center of the island shows the location of the Cañadas caldera wall.

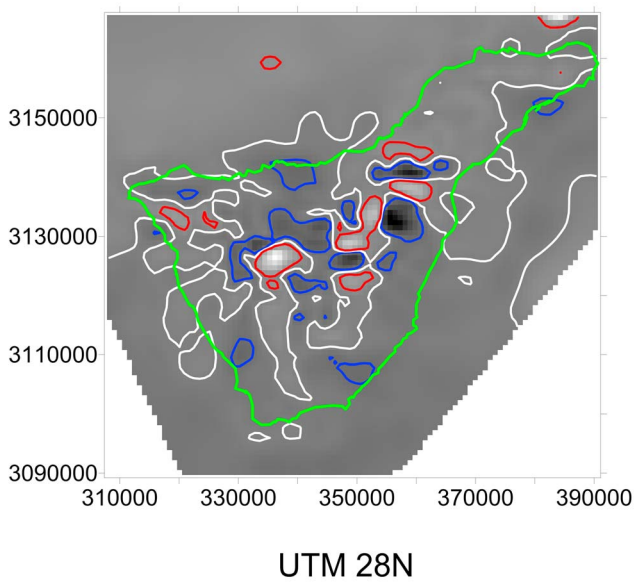

Figure 10. Differences between the measured and the synthetic magnetic fields (produced by the model shown in Figures 8 and 9). The white contour represents a difference of 0 nT, the red contour represents a difference of +100 nT, and the blue contour represents a difference of −100 nT. The gray background indicates the sign of the differences in a certain area: light gray indicates positive differences, whereas dark gray implies negative differences.

the value that provided the best fit between the observed and the synthetic anomalies (Figure 10).

6. Discussion

[40] The interpretation of magnetic anomaly data suffers from limitations that make it unattainable to unambiguously image the geological structures [*Blakely*, 1995]. The greatest uncertainty regards the estimation of the thickness variations of the sources. For instance, the same magnetic anomaly can be reproduced either by a strongly magnetized, small, deep body, or by a weakly magnetized, wide, shallow body. When no additional geological or geophysical constraints are available, it is impossible to identify which of these two scenarios is the best approximation to the geology solely by modeling the magnetic anomaly.

[41] Because no information about the bulk magnetization of intrusive bodies is available for Tenerife, we chose to approach magnetic inversion by searching two "boundary" models, each based on different assumptions. For the first approach (linear inversion) we set the source geometry (one layer made up of prisms of varying height) and explored the magnetization as the unknown parameter (model 1, Figure 6). In the second approach (nonlinear inversion), we set a constant magnetization value for the source and explored its geometry by turning on or off the magnetization within a given geometrical shape (model 2, Figures 8 and 9). Both models fit the magnetic anomaly data of Tenerife and, for that reason, they must be considered equivalent, although each of them enhances one particular aspect of the island's geology.

[42] It is important to emphasize that the horizontal position of lateral magnetization contrasts revealed by both models is coherent. The main difference between the models is that in the linear case, we found the location of lateral magnetization contrast with no information about their depth or vertical extension; whereas in the nonlinear case, we investigated the depth and thickness of the main magnetic sources as a function of magnetization, for different constant magnetization values set a priori. In the second approach, we assumed that the main magnetic sources were magnetized with normal polarity. The linear case demonstrates that most of the volume of Tenerife is characterized by a normal polarity. However, this also implies that the nonlinear model cannot completely fit all of the observed magnetic anomalies, since they also contain the effect of reversely magnetized structures. In spite of this, it can be noted that the model partially accounts for negative magnetization contrasts by assigning null magnetization to some cells.

[43] In the magnetic model shown in Figure 6, the magnetization obtained for each vertical prism represents an average value for the whole prism volume, from the topography to its base, located at a depth of 4 km below sea level. This kind of modeling is useful for imaging lateral magnetization contrasts inside the volcanic edifice. Since the topography has been considered as part of the definition of the magnetic source volume, this method helps us identify magnetic sources that are not simply due to the magnetic effect of a rugged relief.

[44] In fact, the first thing that can be noted is that a uniformly magnetized volcanic edifice cannot account for the magnetic anomalies measured in Tenerife. Moreover, our magnetic model reveals intense magnetization contrasts within the island, especially in the central part of its northern half. These strongly magnetized structures can be interpreted as intrusive complexes that are related to the mafic core of the island and to the vertical dike swarms that fed the volcanic activity of central Tenerife. It is interesting to note that the location of these structures is in correspondence with the part of the volcanic edifice that has undergone the greatest growth. It is reasonable to think that the high magnetization values obtained in this area are related to a very high dike concentration, as a consequence of magma intrusion over a long period of time ranging from the formation of the central basaltic shield until the construction of the Teide-Pico Viejo complex in recent times.

6.1. Correlations Between Surface Paleomagnetic Polarities and Magnetic Models

[45] In order to find out whether the magnetization distribution obtained from linear inversion of the magnetic anomalies is coherent with surface magnetic polarities, we have compared our model with the paleomagnetic polarities measured by *Carracedo* [1979] and shown in Figure 7. To simplify this comparison, we have superimposed the main reverse polarity areas taken from Figure 7 on our magnetic model (Figure 6a).

[46] It can be noted that most of the areas that are characterized by a negative (reverse) magnetization value in our model correspond to areas of reverse surface paleomagnetic polarities. The most significant exception to this correlation can be noticed in the south and southeast of the island. The

magnetic model displays negative magnetization values in this area. However, the surface polarity map shows that reverse polarities in the southern half of Tenerife are mainly restricted to the southwest (area H). This result allows us to deduce that the bulk of the southern volcanic edifice, which corresponds with the central basaltic shield in its deepest portion and the later Cañadas edifice on top of the former, is reversely magnetized. The most recent chronology available for the Cañadas edifice is the one published by *Ancochea et al.* [1999]. They distinguish three phases in the formation of this volcano, named Cañadas I (3.5–2.7 Ma), Cañadas II (2.3–1.4 Ma) and Cañadas III (1.1–0.17 Ma). If we compare these ages with the astronomical polarity time scale (APTS) for the Pliocene and the Pleistocene [*Cande and Kent*, 1995] we can note that the Cañadas I phase corresponds to the normal polarity Gauss chron (2.60–3.58 Ma), whereas the Cañadas II and the lower Cañadas III phases took place during the reverse Matuyama chron (0.78–2.60 Ma). The bulk reverse magnetization revealed by our magnetic model in this area suggests that rocks attributed to these two phases of the Cañadas edifice evolution must be the most significant ones in terms of volume.

[47] In the area of the Anaga peninsula and the Dorsal ridge, the correlation between the magnetization sign in our model and surface paleomagnetic polarities is remarkable. For instance, the magnetic model shows that most of the volume of the Anaga basaltic edifice, in the northeastern corner of the island, is magnetized with a reverse polarity, in clear correlation with surface paleomagnetic data. The most recent work dealing with the magnetic stratigraphy of the basaltic shield volcanoes of Tenerife has revealed that two different magnetozones can be distinguished in the Anaga edifice: a lower magnetozone, characterized by a normal polarity, with an estimated age in the range between 4.89 ± 0.07 and 4.72 ± 0.07 Ma; and an upper magnetozone, with reverse polarity, and ages ranging between 4.39 ± 0.06 Ma and 3.95 ± 0.06 Ma [*Guillou et al.*, 2004]. The results of our magnetic modeling suggest that, in Anaga, the volume of lavas erupted during periods of time characterized by a reverse polarity of the Earth's magnetic field is larger than the volumes emplaced during normal polarity chrons. Taking into account the magnetic chronology proposed by *Guillou et al.* [2004], this means that the upper reverse magnetozone forms the bulk of the Anaga volcano, confirming that most of its growth took place during the Gilbert reverse polarity chron. Our model shows that normal polarities in depth are restricted to the northern part of the edifice.

[48] In the northwestern corner of Tenerife, the Teno basaltic edifice is mainly characterized by normal polarity magnetizations. Reverse magnetic polarities are restricted to the southwestern canyons, as can also be noted in the surface polarity map (area J in Figure 6a). This result is also confirmed by the paleomagnetic investigations carried out by *Leonhardt and Soffel* [2006]. They showed that lavas from the initial phase of subaerial growth of the Teno edifice are reversely magnetized and were formed during the inverse chron C3An.1r lasting from 6.27 to 6.14 Ma [*Cande and Kent*, 1995]. In addition, they concluded that the construction of the bulk of Teno spanned 1.2 Myr and took place during the normal polarity magnetic chrons C3An.1n (between 6.14 and 5.89 Ma) and C3n.4n (between 5.23 and 4.98 Ma), with a hiatus in volcanic activity during the reverse chron C3n.4r (between 5.89 and 5.23 Ma). Our magnetic model is in agreement with this magnetic chronology, as it shows that most of the edifice is characterized by a normal polarity. It also reveals that two main normally magnetized structures can be distinguished in the central part of Teno, suggesting that two intrusive bodies are present inside the edifice.

[49] In the Dorsal edifice, the magnetic model reveals both normal and reverse magnetizations, which, in most cases, correlate quite well with surface paleomagnetic polarities (areas B, C, and E in Figure 6a). The exception is area D, where our model displays normal magnetizations in disagreement with a predominant reverse paleomagnetic polarity in this zone. This difference implies that, beneath the reversely magnetized outcropping materials, there must be an important volume of rocks that were emplaced during a normal polarity magnetic chron. It is worth noting that the highest values of negative magnetization on the entire island appear in correspondence with the highest topography of the Dorsal edifice (area C). We can interpret this structure as one of the dike systems that fed the volcanic activity of this edifice. *Ancochea et al.* [1990] reported ages in the interval between 0.90 and 0.48 Ma for the materials of the Dorsal edifice. Our results indicate that volcanic structures located in areas B, C, and E, were emplaced in the Matuyama, which means that the age of the Dorsal must be of at least 0.78 Ma in order to justify the presence of reverse polarities.

6.2. Deep Magnetic Structure and Rift Zones

[50] The growth of a volcanic island is linked to the intrusion of significant volumes of magma in the form of dikes, sills, etc., from which there is a fraction that reaches the surface. It is therefore reasonable to think that the resulting intrusive complexes mostly developed in the areas where the volcanic island has undergone the most significant growth. In fact, looking at the magnetic model of Tenerife of Figure 6, we can see that the most intense magnetizations are found over the highest areas of the island: in the vicinity of the Cañadas caldera, the Teide-Pico Viejo complex, and the Dorsal edifice. In particular, the Teide-Pico Viejo complex is related to a strongly magnetized structure, centered slightly to the west of the Pico Viejo volcano. We can interpret this strong magnetization as the result of the high density of feeding dikes in this area. It is worth noting that the recent reactivation of the island, occurring in 2004, took place in this part of Tenerife (see Figure 1b) [*Martí et al.*, 2009]. This suggests that the ascent of magma in this area has spanned millions of years, beginning with the early phases of basaltic shield volcanism in central Tenerife and lasting until the building of Teide and Pico Viejo stratovolcanoes, including historic volcanic activity.

[51] High magnetizations are also displayed in the Orotava valley and to the east of the Cañadas caldera wall. It is likely that these strongly magnetized structures are also imaging the magmatic feeding system of the central edifice. In section 6.3 we analyze the link between these structures and flank collapses.

[52] The constant magnetization model (Figures 8 and 9) shows a 3-D magnetic image of Tenerife that completes our

view of the inner structure of the island obtained through linear inversion (Figure 6). This approach is aimed at imaging the main sources of the magnetic anomaly field of Tenerife, assuming that these bodies are characterized by a constant magnetization, and provides us with information about the vertical extent of magnetic structures. This model shows that major intrusive structures in Tenerife are concentrated beneath the northern half of the island. These structures can be interpreted as the mafic core of the island, emplaced during the early phases of growth of Tenerife, and the intrusive complexes that fed later activity in the evolution of the island, the shallowest part of which is shown in more detail in Figure 6. The depth to the bottom of these structures depends on the magnetization value used for the inversion. But in all cases, we note that the main intrusive structure is the body located slightly to the northwest of the Teide-Pico Viejo complex, with a bottom reaching several kilometers below sea level.

[53] The shape of these bodies shows that they are aligned along the E-W direction. This result is of great importance, since this alignment could be related to a major old tectonic feature, active during the early formation of Tenerife, and hardly identified on the surface. Most works dealing with the tectonics of Tenerife only mention two main trends (following ENE-WSW and NW-SE directions) characterizing the subaerial volcanism [e.g., *Martí et al.*, 1996]. It is worth noting that *Marinoni and Gudmundsson* [2000], by studying dikes of the old massifs of Tenerife, found an E-W trend in the Anaga edifice which they related with a major tectonic feature of the Canary region. Our magnetic model agrees with this interpretation and suggests that an E-W fracture was present in the crust beneath Tenerife and played a crucial role during the early formation of the island.

[54] The geometry of deep intrusive bodies in Tenerife has important implications for the understanding of the rift zone structure of the island. The first conclusion that can be outlined is that our magnetic model does not support the hypothesis of a triple rift structure due to hot spot-induced doming proposed by *Carracedo* [1994] for Tenerife, since deep intrusive complexes are not arranged following the isotropic stellate geometry typical of that kind of system. Our model agrees better with the idea of asymmetric rifting, in which two rift arms are more developed than the third one. *Walter and Troll* [2003] concluded that this situation is typical of centrally supplied volcanoes which experience increasing instability of a sector, with the less developed rift zone located in the stable part of the volcano and the stronger rifts located tangential to the creeping sector.

[55] The link between flank collapses and rift zones is commonly accepted. In many ocean island volcanoes, the typical triple rift structure is enhanced by landslides that propagate perpendicular to rift axes [*Moore et al.*, 1989]. However, in some islands an uneven distribution of landslides is observed. *Masson et al.* [2002] stated that, once established, an unstable flank becomes a weakness that favors the future occurrence of collapses in that area. They proposed that failures may be most easily initiated on the island flanks that have the greatest gravitational potential for movement. Then, the removal of part of the island volume through flank failure would depressurize the magmatic system, favoring the concentration of eruptive activity in the vicinity of the landslide scar. The growth of this part of the volcanic island may cause a subsequent gravitational destabilization of the edifice in this area and lead to more collapses of the same flank. This model seems to fit the case of Tenerife, where, with the exception of the Güímar collapse, all the other landslides have been directed northward, dismantling the northern flank of the island.

[56] In summary, we can say that the deep magnetic structure of Tenerife agrees well with this model of asymmetric rifting, since it reveals that intrusive complexes are not present beneath the entire island, but only beneath the flank that has experienced the most important growth. This interpretation also implies that rift zones in Tenerife were not present since the early formation of the island, but are the result of the growth of the volcanic edifice itself.

6.3. The Magnetic Signature of Giant Collapses

[57] The highest magnetization values of our magnetic model, displayed mainly in the northern half of Tenerife, seem to be arranged with a round geometry. In Figure 6b we emphasize that particular shape by superimposing some of the scars corresponding to the different gravitational collapses proposed by other authors (shown in Figure 2). In the Icod and Orotava valleys, this correlation is especially remarkable.

[58] This particular geometry of the strongly magnetized structures in the north of Tenerife could be related to the intrusion of magma through rim faults favored by the decompression resulting from the occurrence of flank collapses. This phenomenon has also been observed in the island of Stromboli [*Tibaldi*, 2001, 2004]. In Tenerife, this kind of event has dismantled the northern part of the island several times. Also, the magnetization contrast between volcanic structures excavated by the landslides and less magnetized volcanic materials (debris avalanche deposits, pyroclastites) that filled the scars is expected to contribute in part to the observed magnetic anomalies.

[59] In section 2.3, we present theories proposed by different authors about the areas involved in each collapse and the location of the corresponding scars. The most controversial of these landslides is the one affecting the Icod valley, since some authors ascribed the origin of the Cañadas caldera to this event [e.g., *Cantagrel et al.*, 1999], in disagreement with those who believe that the caldera was formed by vertical collapses produced by explosive eruptions [e.g., *Martí and Gudmundsson*, 2000].

[60] The curved shape of the strongly magnetized bodies revealed in the area of the Icod valley roughly follows the headwall of the Icod landslide proposed by *Ablay and Hürlimann* [2000] and *Hürlimann et al.* [2004] (see Figure 6b). In fact, the highest magnetization values appear in the vicinity of Teide and Pico Viejo. If we interpret these structures as high-density dike systems, then our result would suggest that the scar of the Icod collapse is buried beneath the slopes of the Teide-Pico Viejo complex. This interpretation is in disagreement with the theory of *Cantagrel et al.* [1999], who placed the scar of the Icod collapse in correspondence with the southern wall of the Cañadas caldera. Moreover, the construction of the Teide-Pico Viejo volcano in this part of the island could be explained by magma rising through rim fractures generated by the collapse. This hypothesis was also proposed by *Ablay and Hürlimann* [2000]. In addition, *del Potro et al.* [2009],

using finite element modeling of the basement beneath Teide, deduced that the Teide edifice was emplaced on the headwall of the Icod landslide. Our results seem to support this idea.

[61] In the area of La Orotava valley, we propose a similar interpretation for the geometry of highly magnetized structures, although our magnetic model does not allow us to distinguish whether this part of the volcanic edifice collapsed only once, or many times, as proposed by *Ablay and Hürlimann* [2000]. Again, the geometry of highly magnetized structures displays a shape that is coherent with the headwall of the Orotava landslide. Therefore, it seems that the intrusion of dikes in this area could be also related to the occurrence of flank collapses. In addition, the reversely magnetized area interpreted as a high-density dike system in the Dorsal edifice (area C in Figure 6a) coincides with the highest part of the Güímar collapse headwall, so a similar interpretation could be applied in this case.

[62] The old basaltic shields of Anaga and Teno were also partially destroyed due to flank collapses. The Anaga edifice is characterized by a low magnetization, which is mostly of reverse polarity. It can be noted that two normal polarity structures are located in the northern part of the edifice, in conjunction with the collapse scar proposed by *Hürlimann et al.* [2004]. In the case of Teno, the location of the main magnetized structures is also coherent with the location of the headwalls of the identified landslides (see Figure 6b).

7. Summary and Conclusions

[63] Potential field anomalies, especially magnetic anomalies, are revealed as a useful tool for improving our knowledge about the inner structure of volcanic islands. The main magnetic sources can be interpreted as deep plutonic complexes, related to the mafic core, emplaced during the early history of the islands. Strong magnetic sources can also indicate dike systems responsible for the growth of the island in later stages. One of the advantages of magnetic data over gravity data is the possibility of obtaining chronological information about the different volcanic phases by comparing magnetic polarities of source bodies with the geomagnetic polarity time scale. In addition, airborne magnetic surveys allow a regularly distributed sampling of the magnetic signal of the whole volcanic edifice, including its submarine portion.

[64] In comparison with previous work in this field [*Araña et al.*, 2000], this study generated more realistic and complex models of the inner structure of Tenerife. These improvements are made possible by the more complete, fresh geochronological and geological frameworks now available, together with the use of advanced 3-D magnetic inversion techniques and high-quality data.

[65] Two different inverse modeling techniques have been applied to Tenerife: (1) a linear inversion method aimed at imaging lateral magnetization contacts, and useful for characterizing the magmatic feeding system of the different volcanic edifices of the island (Figure 6), and (2) a nonlinear inversion method aimed at obtaining a 3-D description of the geometry of deep intrusive bodies, in which a constant magnetization value is assumed to characterize the main magnetic sources (Figures 8 and 9). The obtained models must be understood as two different ways of representing the same geological situation. It is important to bear in mind that magnetic modeling is limited by the ambiguity in the definition of the vertical extent of the sources (i.e., the same magnetic anomaly can be reproduced both by changing magnetization in a layer of constant thickness or by varying the vertical extension of a homogeneously magnetized body). The actual inner structure of Tenerife is surely a compromise between these two perspectives, with both lateral and vertical magnetization contrasts present inside the volume of the island.

[66] The main conclusions of this study can be summarized as follows:

[67] 1. In Tenerife, deep intrusive structures are located beneath the northern part of the island and aligned along the E-W direction. This alignment reveals a major tectonic feature that was active during the early formation of Tenerife and is not evident at the surface.

[68] 2. The arrangement of intrusive bodies does not support the hypothesis of a three-armed rift system that has been present since the early formation of the island, as previously proposed by *Carracedo* [1994]. Instead, our results show that intrusion complexes are located beneath the NW-SE and NE-SW rift arms, in conjunction with the island flank that has undergone the most significant growth, including the occurrence of recurrent northward directed collapses. Therefore, the deep structure of Tenerife agrees better with the theory of asymmetric rifting proposed by *Masson et al.* [2002] for this island. In addition, this interpretation would suggest that rift zones developed as a result of the evolution of the island and appeared during a later stage of growth.

[69] 3. The shallow portion of the intrusive structures show a round geometry that agrees with the location of some of the landslide headwalls previously proposed. This suggests that collapse scars have acted as preferential sites for magma upwelling, explaining why the growth of Tenerife has especially developed the northern flank of the island. In particular, our magnetic model is likely providing the first geophysical evidence of the location of the headwall of the Icod landslide beneath the Teide-Pico Viejo complex, previously proposed by *Ablay and Hürlimann* [2000] and *Hürlimann et al.* [2004]. Therefore, magnetic data would support the vertical collapse hypothesis for the origin of the Cañadas caldera [*Martí and Gudmundsson*, 2000] instead of the landslide hypothesis, which places the Icod collapse scar in conjunction with the southern caldera wall [*Cantagrel et al.*, 1999].

[70] 4. The greatest intrusive complex of all is located beneath the northwest part of the Teide-Pico Viejo complex. This suggests the presence of a very high dike density in this area, resulting from the intrusion of magma spanning millions of years, since the early phases of basaltic shield volcanism in central Tenerife until more recent phases, including the building of Teide and Pico Viejo stratovolcanoes. It is also worth noting that the recent reactivation of the island, occurring in 2004, took place in this area.

[71] **Acknowledgments.** This work was funded by the Ministry of Education and Science of Spain through projects CGL2004-21643-E (TEGETEIDE), CGL2008-03874 (VOLRESTE), and CGL2006-02514.

The participation of I. Blanco-Montenegro was funded by the Istituto Nazionale di Geofisica e Vulcanologia of Italy, through the FIRB-MIUR Project RBPR05B2ZJ. The authors are grateful to Jean-François Lénat, Laurent Michon, and an anonymous reviewer for their constructive comments and suggestions.

References

Ablay, G. J., and M. Hürlimann (2000), Evolution of the north flank of Tenerife by recurrent giant landslides, *J. Volcanol. Geotherm. Res.*, *103*, 135–159, doi:10.1016/S0377-0273(00)00220-1.

Ablay, G. J., and J. Martí (2000), Stratigraphy, structure, and volcanic evolution of the Pico Teide-Pico Viejo formation, Tenerife, Canary Islands, *J. Volcanol. Geotherm. Res.*, *103*, 175–208, doi:10.1016/S0377-0273(00)00224-9.

Almendros, J., J. M. Ibáñez, E. Carmona, and D. Zandomeneghi (2007), Array analyses of volcanic earthquakes and tremor recorded at Las Cañadas caldera (Tenerife Island, Spain) during the 2004 seismic activation of Teide volcano, *J. Volcanol. Geotherm. Res.*, *160*, 285–299, doi:10.1016/j.jvolgeores.2006.10.002.

Ancochea, E., J. M. Fúster, E. Ibarrola, A. Cendrero, J. Coello, F. Hernán, J. M. Cantagrel, and C. Jamond (1990), Volcanic evolution of the island of Tenerife (Canary Islands) in light of new K-Ar data, *J. Volcanol. Geotherm. Res.*, *44*, 231–249, doi:10.1016/0377-0273(90)90019-C.

Ancochea, E., J. L. Brändle, and M. J. Huertas (1995), Alineaciones de centros volcánicos en la isla de Tenerife, *Geogaceta*, *17*, 56–59.

Ancochea, E., M. J. Huertas, J. M. Cantagrel, J. Coello, J. M. Fúster, N. Arnaud, and E. Ibarrola (1999), Evolution of the Cañadas edifice and its implications for the origin of the Cañadas Caldera (Tenerife, Canary Islands), *J. Volcanol. Geotherm. Res.*, *88*, 177–199, doi:10.1016/S0377-0273(98)00106-1.

Araña, V., A. G. Camacho, A. García, F. G. Montesinos, I. Blanco, R. Vieira, and A. Felpeto (2000), Internal structure of Tenerife (Canary Islands) based on gravity, aeromagnetic and volcanological data, *J. Volcanol. Geotherm. Res.*, *103*, 43–64, doi:10.1016/S0377-0273(00)00215-8.

Bear, G. W., H. J. Al-Shukri, and A. J. Rudman (1995), Linear inversion of gravity data for 3-D density distribution, *Geophysics*, *60*, 1354–1364, doi:10.1190/1.1443871.

Blakely, R. J. (1995), *Potential Theory in Gravity and Magnetic Applications*, 441 pp., Cambridge Univ. Press, New York, doi:10.1017/CBO9780511549816.

Blanco-Montenegro, I., J. M. Torta, A. García, and V. Araña (2003), Analysis and modelling of the aeromagnetic anomalies of Gran Canaria (Canary Islands), *Earth Planet. Sci. Lett.*, *206*, 601–616, doi:10.1016/S0012-821X(02)01129-9.

Blanco-Montenegro, I., F. G. Montesinos, A. García, R. Vieira, and J. J. Villalaín (2005), Paleomagnetic determinations on Lanzarote from magnetic and gravity anomalies: Implications for the early history of the Canary Islands, *J. Geophys. Res.*, *110*, B12102, doi:10.1029/2005JB003668.

Blanco-Montenegro, I., I. Nicolosi, A. Pignatelli, and M. Chiappini (2008), Magnetic imaging of the feeding system of oceanic volcanic islands: El Hierro (Canary Islands), *Geophys. J. Int.*, *173*, 339–350, doi:10.1111/j.1365-246X.2008.03723.x.

Bravo, T. (1962), El circo de Las Cañadas y sus dependencias, *Bol. Real Soc. Esp. Hist. Nat.*, *40*, 93–108.

Brown, R. J., and M. J. Branney (2004), Event-stratigraphy of a caldera-forming ignimbrite eruption on Tenerife: The 273 ka Poris formation, *Bull. Volcanol.*, *66*, 392–416, doi:10.1007/s00445-003-0321-y.

Cande, S. C., and D. V. Kent (1995), Revised calibration of the geomagnetic polarity timescale for the late Cretaceous and Cenozoic, *J. Geophys. Res.*, *100*, 6093–6095, doi:10.1029/94JB03098.

Cantagrel, J. M., N. O. Arnaud, E. Ancochea, J. M. Fúster, and M. J. Huertas (1999), Repeated debris avalanches on Tenerife and genesis of the Las Cañadas caldera wall, *Geology*, *27*, 739–742, doi:10.1130/0091-7613(1999)027<0739:RDAOTA>2.3.CO;2.

Carracedo, J. C. (1979), Paleomagnetismo e historia volcánica de Tenerife, report, 81 pp., Aula de Cultura del Cabildo Insular de Tenerife, Santa Cruz de Tenerife, Spain.

Carracedo, J. C. (1994), The Canary Islands: An example of structural control on the growth of large oceanic-island volcanoes, *J. Volcanol. Geotherm. Res.*, *60*, 225–241, doi:10.1016/0377-0273(94)90053-1.

Carracedo, J. C., E. Rodríguez Badiola, H. Guillou, M. Paterne, S. Scaillet, F. J. Pérez Torrado, R. Paris, U. Fra-Paleo, and A. Hansen (2007), Eruptive and structural history of Teide volcano and rift zones of Tenerife, Canary Islands, *Geol. Soc. Am. Bull.*, *119*, 1027–1051, doi:10.1130/B26087.1.

Carracedo, J. C., H. Guillou, E. Rodríguez Badiola, F. J. Pérez-Torrado, A. Rodríguez González, R. Paris, V. Troll, S. Wiesmaier, A. Delcamp, and J. L. Fernández-Turiel (2009), La dorsal NE de Tenerife: Hacia un modelo del origen y evolución de los rifts de islas oceánicas, *Estud. Geol.*, *65*, 5–47, doi:10.3989/egeol.39755.056.

Coello, J. (1973), Las series volcánicas en subsuelos de Tenerife, *Estud. Geol.*, *29*, 491–512.

Coppo, N., P.-A. Schnegg, W. Heise, P. Falco, and R. Costa (2008), Multiple caldera collapses inferred from the shallow electrical resistivity signature of the Las Cañadas caldera, Tenerife, Canary Islands, *J. Volcanol. Geotherm. Res.*, *170*, 153–166.

del Potro, R., H. Pinkerton, and M. Hürlimann (2009), An analysis of the morphological, geological and structural features of Teide strato-volcano, Tenerife, *J. Volcanol. Geotherm. Res.*, *181*, 89–105, doi:10.1016/j.jvolgeores.2008.12.013.

Dóniz, J., C. Romero, E. Coello, C. Guillén, N. Sánchez, L. García-Cacho, and A. García (2008), Morphological and statistical characterisation of recent mafic volcanism on Tenerife (Canary Islands, Spain), *J. Volcanol. Geotherm. Res.*, *173*, 185–195, doi:10.1016/j.jvolgeores.2007.12.046.

Fúster, J. M., V. Araña, J. L. Brändle, M. Navarro, U. Alonso, and A. Aparicio (1968), *Geología y Vulcanología de las Islas Canarias, Tenerife*, 218 pp., Inst. Lucas Mallada, CSIC, Madrid.

García, A., J. Vila, R. Ortiz, R. Maciá, R. Sleeman, J. M. Marrero, N. Sánchez, M. Tárraga, and A. M. Correig (2006), Monitoring the reawakening of Canary Islands' Teide volcano, *Eos Trans. AGU*, *87*(6), 61.

García, A., M. Chiappini, I. Blanco-Montenegro, R. Carluccio, F. D'Ajello Caracciolo, R. De Ritis, I. Nicolosi, A. Pignatelli, N. Sánchez, and E. Boschi (2007), High resolution aeromagnetic anomaly map of Tenerife, Canary Islands, *Ann. Geophys.*, *50*, 689–697.

Geyer, A., and J. Martí (2010), The distribution of basaltic volcanism on Tenerife, Canary Islands: Implications on the origin and dynamics of the rift systems, *Tectonophysics*, *483*, 310–326, doi:10.1016/j.tecto.2009.11.002.

Gottsmann, J., L. Wooller, J. Martí, J. Fernández, A. G. Camacho, P. J. Gonzalez, A. Garcia, and H. Rymer (2006), New evidence for the reawakening of Teide volcano, *Geophys. Res. Lett.*, *33*, L20311, doi:10.1029/2006GL027523.

Gottsmann, J., A. G. Camacho, J. Martí, L. Wooller, J. Fernández, A. García, and H. Rymer (2008), Shallow structure beneath the Central Volcanic Complex of Tenerife from new gravity data, *Phys. Earth Planet. Inter.*, *168*, 212–230, doi:10.1016/j.pepi.2008.06.020.

Guillou, H., J. C. Carracedo, R. Paris, and F. Pérez-Torrado (2004), Implications for the early shield-stage evolution of Tenerife from K/Ar ages and magnetic stratigraphy, *Earth Planet. Sci. Lett.*, *222*, 599–614, doi:10.1016/j.epsl.2004.03.012.

Huertas, M. J., N. O. Arnaud, E. Ancochea, J. M. Cantagrel, and J. M. Fúster (2002), $^{40}Ar/^{39}Ar$ stratigraphy of pyroclastic units from the Cañadas Volcanic Edifice (Tenerife, Canary Islands) and their bearing on the structural evolution, *J. Volcanol. Geotherm. Res.*, *115*, 351–365, doi:10.1016/S0377-0273(01)00331-6.

Hürlimann, M., E. Turon, and J. Martí (1999), Large landslides triggered by caldera collapse events in Tenerife, Canary Islands, *Phys. Chem. Earth*, *24*, 921–924, doi:10.1016/S1464-1895(99)00136-2.

Hürlimann, M., J. Martí, and A. Ledesma (2004), Morphological and geological aspects related to large slope failures on oceanic islands. The huge La Orotava landslides on Tenerife, Canary Islands, *Geomorphology*, *62*, 143–158, doi:10.1016/j.geomorph.2004.02.008.

Instituto Geológico y Minero de España (2004), *Geología de España*, 884 pp., Inst. Tecnol. Geomin. de Esp., Madrid.

Jackson, D. D. (1972), Interpretation of inaccurate, insufficient and inconsistent data, *Geophys. J. R. Astron. Soc.*, *28*, 97–109.

Lagarias, J. C., J. A. Reeds, M. H. Wright, and P. E. Wright (1998), Convergence properties of the Nelder-Mead simplex method in low dimensions, *SIAM J. Optim.*, *9*, 112–147, doi:10.1137/S1052623496303470.

Leonhardt, R., and H. C. Soffel (2006), The growth, collapse and quiescence of Teno volcano, Tenerife: New constraints from paleomagnetic data, *Int. J. Earth Sci.*, *95*, 1053–1064, doi:10.1007/s00531-006-0089-3.

MacMillan, S., and S. Maus (2005), International geomagnetic reference field-The tenth generation, *Earth Planets Space*, *57*(12), 1135–1140.

Marinoni, L., and A. Gudmundsson (2000), Dykes, faults and paleostresses in the Teno and Anaga massifs of Tenerife (Canary Islands), *J. Volcanol. Geotherm. Res.*, *103*, 83–103, doi:10.1016/S0377-0273(00)00217-1.

Martí, J., and A. Gudmundsson (2000), The Las Cañadas caldera (Tenerife, Canary Islands): An overlapping collapse caldera generated by magma-chamber migration, *J. Volcanol. Geotherm. Res.*, *103*, 161–173, doi:10.1016/S0377-0273(00)00221-3.

Martí, J., J. Mitjavila, and V. Araña (1994), Stratigraphy, structure and geochronology of the Las Cañadas caldera (Tenerife, Canary Islands), *Geol. Mag.*, *131*, 715–727, doi:10.1017/S0016756800012838.

Martí, J., G. J. Ablay, and S. Bryan (1996), Comment on "The Canary Islands: an example of structural control on the growth of large oceanic-

island volcanoes" by J.C. Carracedo, *J. Volcanol. Geotherm. Res.*, *72*, 143–149, doi:10.1016/0377-0273(95)00079-8.

Martí, J., M. Hürlimann, G. J. Ablay, and A. Gudmundsson (1997), Vertical and lateral collapses on Tenerife (Canary Islands) and other volcanic ocean islands, *Geology*, *25*, 879–882, doi:10.1130/0091-7613(1997)025<0879:VALCOT>2.3.CO;2.

Martí, J., R. Ortiz, J. Gottsmann, A. García, and S. De La Cruz-Reyna (2009), Characterising unrest during the reawakening of the central volcanic complex of Tenerife, Canary Islands, 2004–2005, and implications for assessing hazards and risk mitigation, *J. Volcanol. Geotherm. Res.*, *182*, 23–33, doi:10.1016/j.jvolgeores.2009.01.028.

Masson, D. G., A. B. Watts, M. J. R. Gee, R. Urgeles, N. C. Mitchell, T. P. Le Bas, and M. Canals (2002), Slope failures on the flanks of the western Canary Islands, *Earth Sci. Rev.*, *57*, 1–35, doi:10.1016/S0012-8252(01)00069-1.

Moore, J. G., D. A. Clague, R. T. Holcomb, P. W. Lipman, W. R. Normark, and M. E. Torresan (1989), Prodigious submarine landslides on the Hawaiian Ridge, *J. Geophys. Res.*, *94*, 17,465–17,484, doi:10.1029/JB094iB12p17465.

Münn, S., T. R. Walter, and A. Klügel (2006), Gravitational spreading controls rift zones and flank instability on El Hierro, Canary Islands, *Geol. Mag.*, *143*, 257–268, doi:10.1017/S0016756806002019.

Nicolosi, I., I. Blanco-Montenegro, A. Pignatelli, and M. Chiappini (2006), Estimating the magnetization direction of crustal structures by means of an equivalent source algorithm, *Phys. Earth Planet. Inter.*, *155*, 163–169, doi:10.1016/j.pepi.2005.12.003.

Pous, J., W. Heise, P.-A. Schnegg, G. Muñoz, J. Martí, and C. Soriano (2002), Magnetotelluric study of the Las Cañadas caldera (Tenerife, Canary Islands): Structural and hydrogeological implications, *Earth Planet. Sci. Lett.*, *204*, 249–263, doi:10.1016/S0012-821X(02)00956-1.

Press, W. H., S. A. Teukolsky, W. T. Vetterling, and B. P. Flannery (1992), *Numerical Recipes in C: The Art of Scientific Computing*, 2nd ed., 994 pp., Cambridge Univ. Press, New York.

Roest, W. R., J. J. Dañobeitia, J. Verhoef, and B. J. Collette (1992), Magnetic anomalies in the Canary Basin and the Mesozoic evolution of the central North Atlantic, *Mar. Geophys. Res.*, *14*, 1–24, doi:10.1007/BF01674063.

Schmincke, H.-U. (2004), *Volcanism*, 324 pp., Springer, Berlin.

Sharma, P. V. (1986), *Geophysical Methods in Geology*, 432 pp., Elsevier, Amsterdam.

Socías, I., and J. Mézcua (1996), Levantamiento aeromagnético del archipiélago canario, *Publ. Téc. 35*, 28 pp., Inst. Geogr. Nac., Madrid.

Teide Group (1997), Morphometric study of the northwest and southeast slopes of Tenerife, Canary Islands, *J. Geophys. Res.*, *102*, 20,325–20,342, doi:10.1029/97JB01281.

Thirlwall, M. F., B. S. Singer, and G. F. Marriner (2000), ^{39}Ar-^{40}Ar ages and geochemistry of the basaltic shield stage of Tenerife, Canary Islands, Spain, *J. Volcanol. Geotherm. Res.*, *103*, 247–297, doi:10.1016/S0377-0273(00)00227-4.

Tibaldi, A. (2001), Multiple sector collapses at Stromboli volcano, Italy: How they work, *Bull. Volcanol.*, *63*, 112–125, doi:10.1007/s004450100129.

Tibaldi, A. (2004), Major changes in volcano behaviour after a sector collapse: Insights from Stromboli, Italy, *Terra Nova*, *16*, 2–8, doi:10.1046/j.1365-3121.2003.00517.x.

Walter, T. R. (2003), Buttressing and fractional spreading of Tenerife, an experimental approach on the formation of rift zones, *Geophys. Res. Lett.*, *30*(6), 1296, doi:10.1029/2002GL016610.

Walter, T. R., and H. U. Schmincke (2002), Rifting, recurrent landsliding and Miocene structural reorganization on NW-Tenerife (Canary Islands), *Int. J. Earth Sci.*, *91*, 615–628, doi:10.1007/s00531-001-0245-8.

Walter, T. R., and V. R. Troll (2003), Experiments on rift zone evolution in unstable volcanic edifices, *J. Volcanol. Geotherm. Res.*, *127*, 107–120, doi:10.1016/S0377-0273(03)00181-1.

Walter, T. R., V. R. Troll, B. Cailleau, A. Belousov, H.-U. Schmincke, F. Amelung, and P. v. d. Bogaard (2005), Rift zone reorganization through flank instability in ocean island volcanoes: An example from Tenerife, *Bull. Volcanol.*, *67*, 281–291, doi:10.1007/s00445-004-0352-z.

Watts, A. B., and D. G. Masson (1995), A giant landslide on the north flank of Tenerife, Canary Islands, *J. Geophys. Res.*, *100*, 24,487–24,498, doi:10.1029/95JB02630.

Watts, A. B., and D. G. Masson (2001), New sonar evidence for recent catastrophic collapses of the north flank of Tenerife, Canary Islands, *Bull. Volcanol.*, *63*, 8–19, doi:10.1007/s004450000119.

I. Blanco-Montenegro, Departamento de Física, Universidad de Burgos, Escuela Politécnica Superior, Avda. de Cantabria s/n, E-09006 Burgos, Spain. (iblanco@ubu.es)

M. Chiappini, I. Nicolosi, and A. Pignatelli, Istituto Nazionale di Geofisica e Vulcanologia, Via di Vigna Murata 605, I-00143 Roma, Italy.

A. García, Departamento de Volcanología, Museo Nacional de Ciencias Naturales, CSIC, José Gutierrez Abascal 2, E-28006 Madrid, Spain.